Tanzania Journal of Engineering and Technology 2022, **41**(**4**):155-168
OPEN ACCESS articles distributed under Creative Commons Attribution
Licence [CC BY-ND]
Websites: https://ajol.org/tjet; https://tjet.udsm.ac.tz

ISSN 1821-536X (**print**); ISSN 2619-8789 (**electronic**)
DOI: https://doi.org/10.52339/tjet.v41i4.875

Full Length Research Article

Synthesis, Characterisation and Catalytic Evaluation of Castor Oil-Templated Mesoporous Sulfated Solid Acid Catalysts for Esterification Reaction

Stephen S. Nyandoro[1*] and Elianaso Elimbinzi[1,2]

[1]Chemistry Department, College of Natural and Applied Sciences, University of Dar es Salaam P.O. Box 35061, Dar es Salaam, TANZANIA
[2]Department of Chemistry, Faculty of Science, Mkwawa University College of Education, A Constituent College of the University of Dar es Salaam, P.O. Box 2513, Iringa, TANZANIA
[*]Corresponding Author email: nyandoro@udsm.ac.tz; ORCID: https://orcid.org/0000-0002-4659-0187

ABSTRACT

In bio-refinery and other catalytic reactions, heterogeneous catalysts confer advantage over homogenous catalysts due to minimized recovery and separation costs. However, templating surfactant and solid support for the synthesis of heterogeneous catalysts ought to consider their cheap sources and environmentally friendliness for their sustainable use. Thus, with the vision to make the process significantly benign, in the present work, solid acids were synthesised from renewable sources (castor oil as surfactant and rice husk as the source of silica). The synthesised castor oil-templated mesoporous sulfonic acid modified catalysts (SO_3H-MTS and SO_3H-MT-RHS) were characterised and evaluated for catalytic esterification of acetic acid (C2), hexanoic acid (C6), lauric acid (C12), palmitic acid (C16), and ricinoleic acid (C18) with butanol at 110 °C. Physicochemical properties of the synthesised materials were characterised by nitrogen porosimetry, X-ray powder diffraction, thermogravimetry, X-ray Photoelectron Spectroscopy (XPS), and Diffuse Reflectance Infrared Fourier Transform Spectroscopy (DRIFTS). The porosimetric analysis of the synthesised materials revealed a type IV adsorption-desorption isotherm reminiscent of the mesoporous structures. The surface area of the synthesised materials decreased upon functionalisation by sulfonic group. The DRIFTS and XPS confirmed the attachment of sulfonic functional group on the synthesised materials. Evaluation of the catalytic performance of the synthesized materials was determined through analysis of carboxylic acid conversions using gas chromatographic technique. SO_3H-MTS gave higher acid conversions compared to SO_3H-MT-RHS. The sulfated solid acid catalysts showed good catalytic activity on the esterification with conversion ranging from 96-37% for C2-C18 with butanol at 110 °C within 6 h. Such castor oil-templated mesoporous sulphated solid acid catalysts can therefore be applied in biodiesel production upon process optimisation.

ARTICLE INFO

Submitted: **September 27, 2022**

Revised: **December 17, 2022**

Accepted: **December 27, 2022**

Published: **December 30, 2022**

Keywords: *Castor oil-templated mesoporous; sol-gel; solid acid catalysts; esterification; rice husk-derived silica; C2-C18.*

INTRODUCTION

Since early 1990s, there has been a surge of interest in the synthesis of mesoporous materials due to the advantageous properties associated with large surface area, pore size distribution, and pore diameter (Pagar *et al.*, 2018; El Kadib *et al.*, 2013; Beck *et al.*, 1992; Kresge *et al.*, 1992). A surfactant-templated sol-gel system is one of the popular techniques used to synthesise such materials (Che *et al.*, 2003; Zhao *et al.*, 2000; Cheng *et al.*, 1999; Beck *et al.*, 1992; Kresge *et al.*, 1992). The process involve sol-gel technique in which an alkoxide such as tetramethyl orthosilicate (TMOS) or tetraethyl orthosilicate (TEOS) is mixed with a protic solvent such as water, ethanol or methanol to form a solution under alkaline or acidic conditions. Mesoporous silicas produced in this manner have amorphous or crystalline characteristics which provide a degree of flexibility to the overall structural properties of the materials. The presence of silanol groups on the surface of mesoporous silica give wide options for functionalisation and eventual various purposeful applications of the materials (Medina-Juarez *et al.*, 2016; He and Shi 2011). Thus, due to their internal large surface area and other desirable characteristics such materials are used in sorption media, biosensors, biomedical and catalysis (Bharti *et al.*, 2015; Gérardin *et al.* 2013; Hasanzadeh *et al.* 2012; Tang *et al*,. 2012; Ritter *et al.*, 2010).

Different solid acid catalysts such as zirconia, zeolite, nafion montmorillonite K10 or their modified forms have been successfully applied in diverse organic reactions including esterification (Liu *et al.*, 2018 Diamantopoulos 2015; Meghshyam *et al.*, 2011; Jothiramalingam and Wang 2009; López *et al.*, 2008; Reddy *et al.*, 2005). The use of solid acid catalysts for esterification reaction usually results into production of esters including those deployable in biodiesel manufacturing in good yields (Balan *et al.*, 2021; Mendaros *et al.*, 2020; Shagufta *et al.*, 2017; Saravanan *et al.*, 2014; Narkhede and Patel 2013; Park *et al.*, 2010; Kulkarni *et al.*, 2006). However, mesoporous silicas derived from materials such as TEOS are generally expensive (Elimbinzi *et al.*, 2020, 2018; Bhagiyalakshmi *et al.*, 2010), hence there is need for an alternative low cost silica source from agricultural wastes such as rice husk, sugarcane bagasse and wheat husk. The rice husk being known for its higher silica content (Vaibhav *et al.*, 2015), it was chosen for the investigations reported in this work. Conversely, most artificial surfactants such as pluronic acid used in the synthesis of mesoporous materials are environmentally unfriendly. Therefore, it is more appealing to deploy natural surfactants that are not only environmentally friendly but also economically viable and have long-term benefits. In these regards, the dual bio-derived templates prepared from castor oil as source of surfactant and silica derived from rice husk (RHS) as solid support was used to prepare mesoporous solid acids. The investigations also included the development of a mesoporous support using castor oil as a templating agent and TEOS as silica source for comparison purposes. The synthesised solid supports were functionalized with sulfonic acid to form the desired solid acid catalysts. Catalysts synthesised from renewable sources (castor oil as surfactant and rice husk as the source of silica) were envisaged to make the process significantly green. Recently, solid base catalysts prepared using such materials were tested for their catalytic activities on transesterification of triacylglycerols (TAGs) namely tributyrin (C4), tricaprylin (C8) and trilaurin (C12) for biodiesel production in which castor oil templating of RHS increased the mesoporosity and activity of the resulting solid base catalysts (Elimbinzi *et al.*, 2020).

In this work, the use of castor oil-templated silica to synthesize the solid acids SO_3H-MTS and SO_3H-MT-RHS is reported. The synthesized solid acids were subsequently evaluated for their effectiveness in catalytic esterification of acetic (C2), hexanoic (C6), lauric (C12), palmitic (C16) and ricinoleic (C18) acids with butanol at 110 °C.

MATERIALS AND METHODS

Materials and chemicals used

Castor seeds were collected from Iringa region while the rice husks were collected from the local miller at Toangoma in Dar es salaam, Tanzania. Tetraethyl orthosilicate (TEOS) (99.0%), hydrochloric acid (35%), potassium bromide *n*-hexane (<97%), potassium hydroxide (85%), sodium hydroxide (99.0%), magnesium sulfate (99%), 3-mercaptopropyltrimethoxysilane (MPTMS) (97%), dry toluene (>99.5 %), hydrogen peroxide (30%), *tert*-butyl ether (99.5%), dihexyl ether (98%), acetic (C2), hexanoic (C6), lauric (C12), palmitic (C16) acids, butanol (99.5%), ethanol (>99.8%) , methanol (>99.9%), and dichloromethane (99.9%). These chemicals were bought from Sigma Aldrich and used without any further purification.

Extraction of castor oil and isolation of ricinoleic acid

Extraction of castor oil was done as per recently reported method (Elimbinzi and Nyandoro 2021; Elimbinzi *et al.*, 2020). In brief, 10 g of crushed castor seeds were placed in a thimble at the centre of the extractor, and then extracted using 250 mL of *n*-hexane heated at 60 °C for 2 h in a round bottom flask connected to a reflux condenser. The *n*-hexane vapour was condensed and passed through the thimble, then siphoned back to the flask. Castor oil was obtained after evaporation of *n*-hexane using a rotary-evaporator (Heidolph Rotary Evaporator, Laborota 4003). Ricinoleic acid isolation from castor oil was achieved following a protocol developed by Vaisman *et al.* (2008) with some modification as recently reported by Elimbinzi *et al*. (2020). Castor oil (250 g) was hydrolysed by refluxing with potassium hydroxide (60 g) in ethanol (500 mL) for 1 h. Evaporation of ethanol was done then the obtained residue was dissolved in warm distilled water (1.2 L) followed by acidification with concentrated hydrochloric acid up to pH = 1. Ricinoleic acid was extract by mixing *tert*-butyl ether (50 mL) to the acidified mixture. Separating funnel was used to partition the organic layer containing ricinoleic acid from the aqueous layer. The organic layer was washed with warm water (2 L) then dried by magnesium sulphate. Ricinoleic acid was recovered by evaporating the solvent under vacuum using rotary-evaporator.

Preparation of sodium silicate from rice husk ash

Rice husks (20 g) were burnt at high temperature muffle furnace (Model F46120CM) at 600 ºC for 5 h to obtain the rice husk ash (RHA). Rice husk silica was obtained as previously reported (Elimbinzi *et al.*, 2020; Ligate and Mdoe 2013). Thus, 10 g portions of RHA was dissolved in 200 mL of 2 M sodium hydroxide solution followed by boiling for 1 hour and then allowed to cool. The mixture was filtered to obtain sodium silicate solution. The residue was then discarded. Equation 1 shows the formation of sodium silicate from the reaction of rice husk ash and NaOH.

$$SiO_2(Ash)(s) + 2NaOH(aq) ----> Na_2SiO_3(aq) + H_2O(1) \qquad (1)$$

Preparation of mts/mt-rhs and sulfonic acid functionalised mts/mt-rhs

Castor oil (2.5 g) was dissolved in a stirred mixture of 308 mL deionised water and 57 mL of 2 M hydrochloric acid. The resulting mixtures were stirred at 35 °C for 2 h followed by addition of either TEOS or sodium silicate extracted from the rice husk ash (23 mL) as silica source for synthesis of MTS or MT-RHS solid support, respectively, then stirred further at 35 °C for 24 h, prior to aging at 80 °C for 24 h in a closed vessel. The synthesised product was filtered and washed three times with ethanol and dried overnight at room temperature. The organic template was removed by Soxhlet extraction using 200 mL ethanol by refluxing at 70 °C for 10 h. The mesoporous material termed as MTS and MT-RHS for TEOS and rice husk derived mesoporous materials, respectively were obtained after filtration and drying at ambient conditions. MTS and MT-RHS (2 g each) were separately oven dried for 1 hour at 100 °C. The dried materials were dispersed in 60 mL of dry toluene and stirred for 1 hour before adding 1 mL MPTMS (Figure 1). The resulting mixtures were refluxed at 130 °C for 24 hours, filtered, washed with methanol, and then oven dried overnight in at 100 °C. The obtained thiol-functionalised mesoporous materials were termed SH-MTS and SH-MT-RHS. To obtain the solid sulfonic acid, the thiol-functionalised mesoporous silica materials (1 g) were dissolved in 30% H_2O_2 (20 mL) and refluxed for 3 hours. The solid materials were obtained by filtration, methanol washing, and drying at room temperature. The sulfonic functionalised mesoporous material were termed SO_3H-MTS and SO_3H -MT-RHS (Figure 1).

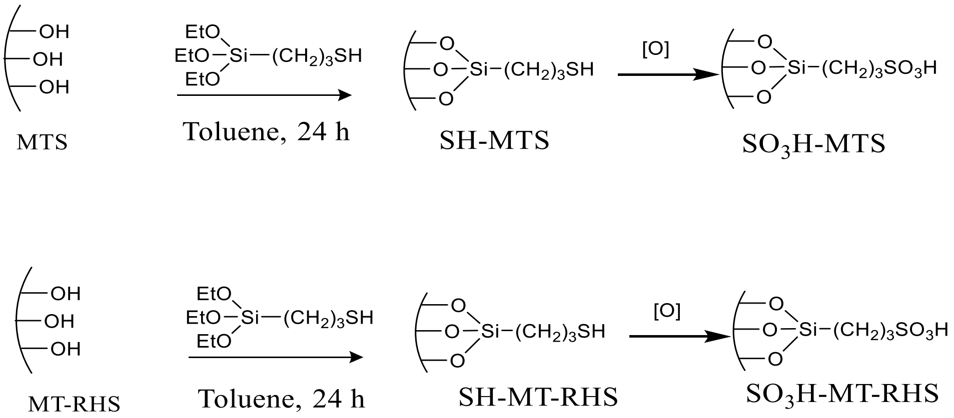

Figure 1: Reaction scheme showing thiol grafted to the MTS/MT-RHS and oxidation of thiol to sulfonic acid.

Characterisation of the synthesised catalysts

N_2 porosimetry was performed on a Quantachrome Nova 4000 porosimeter, with BET surface area calculated over the range P/Po = 0.03-0.19, in which a linear relationship was maintained. The BJH model to the desorption branch of the isotherm were applied to determine the pore size distributions of the synthesised materials. X-ray powder diffraction (XRD) on a Bruker D8 Advance diffractometer using the Cu Kα line in the range $2\theta = 10$-80° with a step size of 0.04° was used to evaluate the structural order with phase identification. Surface elemental composition of the synthesised materials were determined by X-ray Photoelectron Spectroscopy (XPS) using a Kratos Axis HSi spectrometer equipped with a charge neutraliser, a monochromated Al Kα source (1486.7 eV) and magnetic focusing lens. Spectra were recorded at normal emission with the energy of 40 eV under a vacuum of 1.3×10^{-11} kPa, with binding energies referenced to carbon C1s at 284.8 eV. Curve fitting of XPS spectra were obtained using CasaXPS version 2.3.15. Thermogravimetry analysis of the synthesised castor oil-templated mesoporous materials was done using PerkinElmer Pyris 6 TGA thermal analyser. 15 mg of samples were placed into clean sample holders and heated under nitrogen atmosphere with a purge rate of 20 mL/min from 40 °C to 800 °C at a heating rate of 10 °C/minute. Functional groups present in the synthesized materials were identified using Diffuse Reflectance Infrared Fourier Transform Spectroscopy (DRIFTS). The sample was mixed with KBr in 1:9 (w/w ratio). The fine ground mixed sample powder was then placed into a cup-disc for analysis. The FTIR spectra were collected in the 4000-500 cm^{-1} range with a resolution of 4 cm^{-1}, 64-scan number, and the results were obtained by subtracting the KBr background spectrum from the sample spectra. All spectra were reported in absorbance and wave numbers (cm^{-1}).

Evaluation of the catalytic performance

Batch esterification was carried out at 110 °C using a Radleys Carousel Reactor Station in which 150 mmol of butanol, 5 mmol of carboxylic acids [acetic (C2), hexanoic (C6), lauric (C12), palmitic (C16) or ricinoleic (C18) acid] with 0.5 mmol of dihexyl ether (used as an internal standard) and 100 mg of each sulfonic acid functionalised MTS/MT-RHS catalyst was added to the two-neck flask. Samples were collected intermittently, filtered and diluted with dichloromethane then analysed by gas chromatography (GC). Varian 450-GC equipped with a Phenomenex ZB-5HT Inferno 15 m × 0.32 mm × 0.10 µm was used to monitor acetic and hexanoic acid esterification while a 1079 programmable, direct on-column injector and Phenomenex ZB-1 HT Inferno 15 m × 0.53 mm × 0.15 µm capillary column was used for lauric, palmitic and ricinoleic acid esterification. An average of three injections per sample was recorded for all catalytic profiles. Conversions were reported based on the changes in the concentration of the carboxylic acid, with initial rates calculated over the first hour of the reaction.

RESULTS AND DISCUSSION

Materials characterisation

N_2 porosimetry conducted at 77 K was used to study porosity properties of the unmodified MTS/MT-RHS and sulfonic acid modified MTS/MT-RHS. In this study, the BET model was used to determine surface area whereas the pore volume and pore diameter were analysed by BJH approach. All synthesised products displayed type IV isotherm with hysteresis loop indicating capillary condensation of the mesoporous materials (Figure 2 and 3). The BET graphs for N_2 gas adsorption-desorption (Figure 2) showed generally straight lines for MTS/MT-RHS and their acid functionalised catalysts, SO_3H-MTS/SO_3H-MT-RHS.. Figure 2 and 3 indicate the surface area, pore diameter and pore volume of the catalysts decreasing after functionalisation. The nitrogen absorption also decreased upon thiol functionalisation of the MTS. A further decrease was observed upon oxidation of thiols to sulfonic acid MTS/MT-RHS. Such observed decrease in nitrogen adsorption is attributed to the presence of the functional groups occupying the pores, hence evidence for the successful functionalisation of MTS/MT-RHS being in agreement with other studies (Alfawaz *et al*., 2022, Barczak 2019). The textural properties of MTS, thiol and sulfonic acid MTS/MT-RHS catalysts synthesised at different acid loading concentration are summarised in Table 1.

The XRD analysis of the synthesised materials (MTS, MT-RHS, SH-MTS/MT-RHS, and SO_3H-MTS/MT-RHS) revealed the materials were amorphous and lacked long range ordered pores (Figure 4). This was clearly shown by the broader peak observed at around 20° indicating disorders and presence of amorphous silica instead of crystalline form. These were comparable to those observed in a similar study (Elianaso *et al.*, 2018).

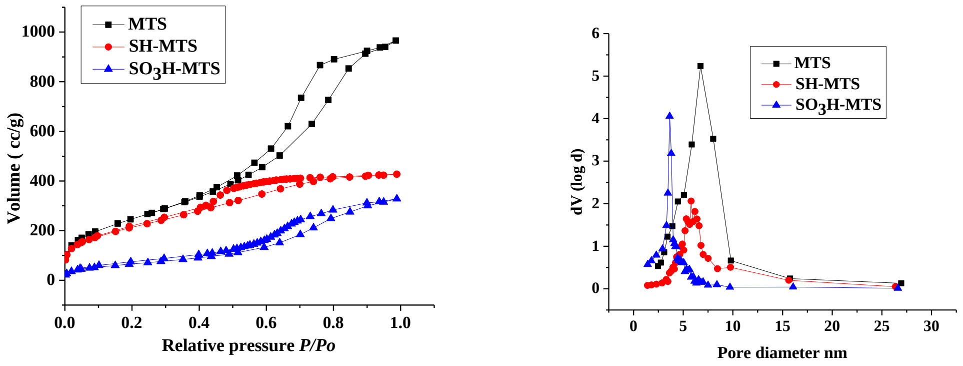

Figure 2: Isotherms and pore size distribution curves for non-functionalised, thiol, and sulfonic acid functionalised MTS.

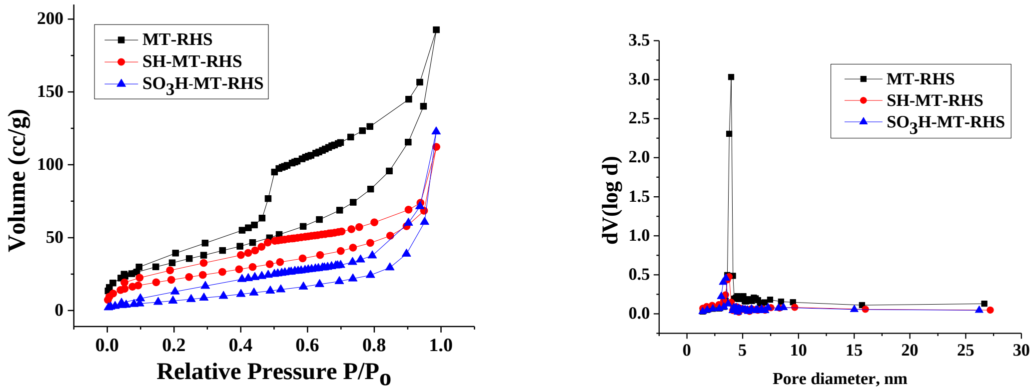

Figure 3: Isotherms and pore size distribution curves for non-functionalised, thiol and sulfonic acid functionalised MT-RHS.

Table 1: Textural properties of the MTS, MT-RHS, and sulfonic acid functionalised MTS/MT-RHS catalysts

ID	**Surface area / m^2 g^{-1}**	**Pore diameter / nm**	**Pore volume /cc g^{-1}**	**Acid/mmol g^{-1}**
MTS	899	6.7	1.47	-
SH-MTS	343	5.8	0.68	-
SO_3H-MTS	218	3.4	0.53	1.73
MT-RHS	192	3.8	0.49	-
SH-MT-RHS	128	3.8	0.12	-
SO_3H-MT-RHS	100	2.3	0.31	0.15

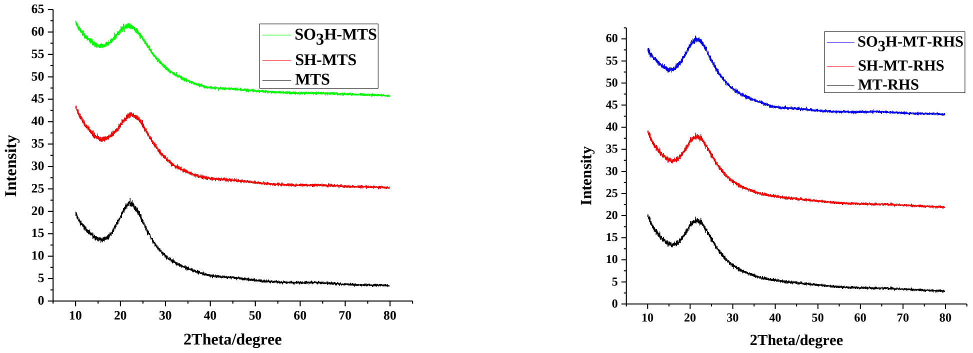

Figure 4: XRD patterns for MTS, MT-RHS, thiol and sulfonic acid functionalised MTS/MT-RHS.

TGA and DTG analysis of all synthesised MTS, MT-RHS, including thiol and sulfonic acid functionalised MTS/MT-RHS indicated weight loss below 100 °C due to adsorbed water, followed by large weight loss for functionalised materials at 300-500 °C due to thiol and sulfonic acid group decomposition (Figure 5 and 6). Further heating above 600 °C resulted in additional weight loss, which was attributed to condensation of the silanol group, which was associated with water loss. Such trends were similar to those observed by Usai *et al.* (2013). Furthermore, when compared to MTS/MT-RHS, the increased weight loss for the thiol and sulfonic functionalised materials at higher temperatures confirmed that the functional groups were anchored to the solid support corroborating observations reported by Melero *et al.* (2010). TGA analysis suggested that all of the synthesised solid supports and catalysts were thermally stable.

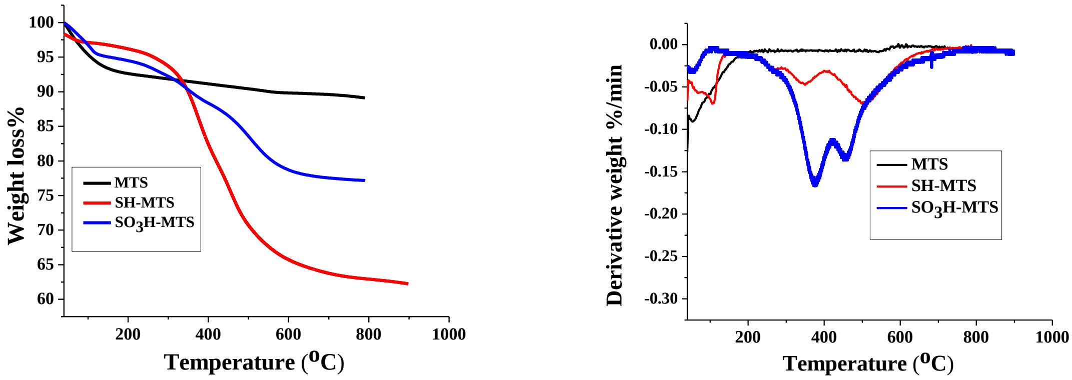

Figure 5: TGA and DTG plots for MTS, thiol, and sulfonic acid functionalised MTS.

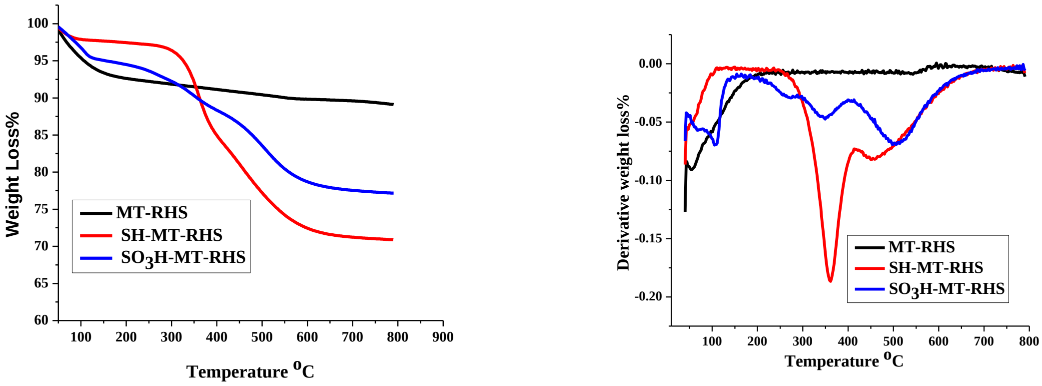

Figure 6: TGA and DTG plots for MT-RHS, thiol, and sulfonic acid functionalised MT-RHS.

The functional groups present in the synthesised solid acid catalysts were confirmed using DRIFTS analysis. The spectrum of unfunctionalised mesoporous materials exhibited silane vibrations around 1067 cm^{-1} due to the presence of Si-O-Si, which is also associated with absorptions at 3569 and 970 cm^{-1} indicating the presence of Si-OH. Materials functionalised with 3-mercaptopropyltrimethoxysilane had a weak vibration band at 2553 cm^{-1}, which corresponded to the S-H functional group. Weak vibration bands corresponding to C-S stretch (Figure 7) were also observed at 687 and 792 cm^{-1}. In the IR spectra of SO_3H-MTS, the absorption bands at 1423 and 1395 cm^{-1} were assigned to S=O of propyl sulfonic acid. The S-H stretching band was observed at 2566 cm^{-1} for thiol functionalised MT-RHS (Figure 7). The lack of an S-H band in the sulfonic acid functionalised MT-RHS indicated that the thiol was oxidised, resulting in an absorption band at 1346 cm^{-1} assigned to the sulfonic acid S=O stretch. Both thiol and sulfonic acid functionalised MT-RHS spectra showed a C-H stretching band at 2934 and 2852 cm^{-1}. The observed functional groups were akin to similar materials (Usai *et al.*, 2013).

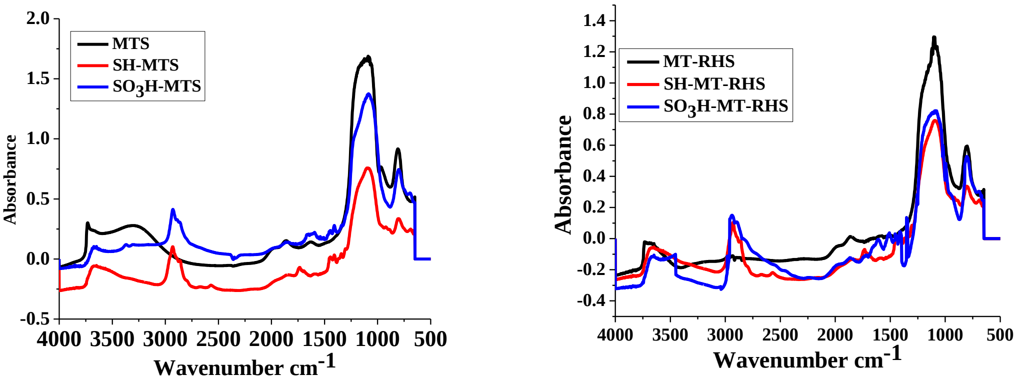

Figure 7: The DRIFT spectra of MTS/MT-RHS, thiol and sulfonic acid functionalised MTS/MT-RHS.

In addition, XPS was performed to analyse the surface elemental/chemical composition of the non-functionalised and functionalised mesoporous silica material. Peaks in the spectrum for non-functionalised mesoporous silica materials corresponded to binding energies of approximately 99.9, 283.2, and 529.3 eV for Si 2p, C 1s, and O 1s, respectively. The presence of S 2p in the XPS spectra for sulfonic acid functionalised MTS/MT-RHS at 168 eV binding energy justified the incorporation of sulfonic acid on the surface of the mesoporous material as shown in Figure 8 and 9. To find the models composed of several peaks under the convoluted peaks representing different chemical states, all of the XPS curves of the non-functionalised and functionalised MTS/MT-RHS were fitted (Alexander *et al.*, 2000; Hughes and Sexton 1988). Based on the XPS spectrum, SO_3H-MTS and SO_3H-MT-RHS were established to have sulfur content percentages of 1.50 and 1.19, respectively.

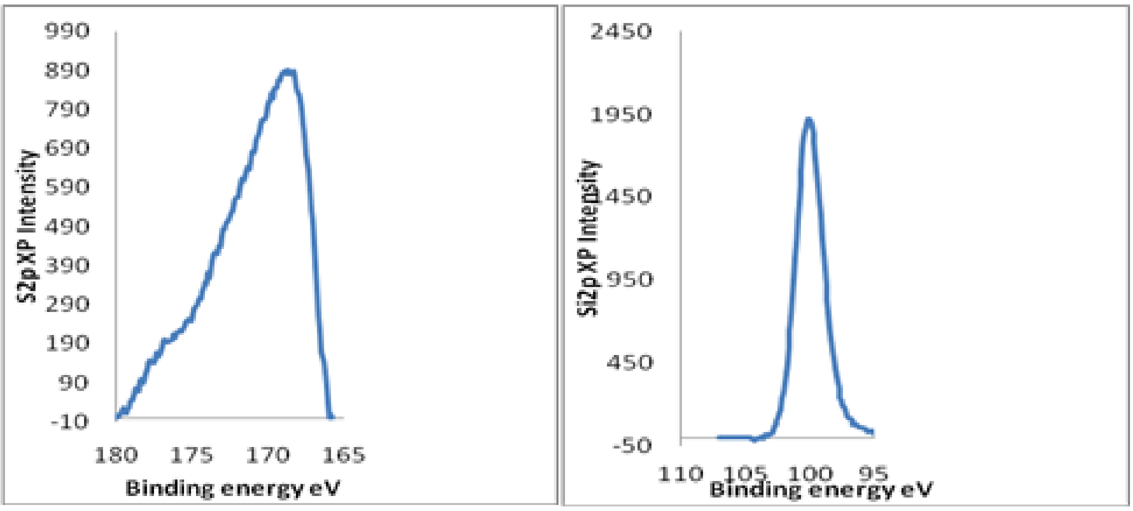

Figure 8: XPS spectra of S 2p and Si 2p for sulfonic acid functionalized MTS.

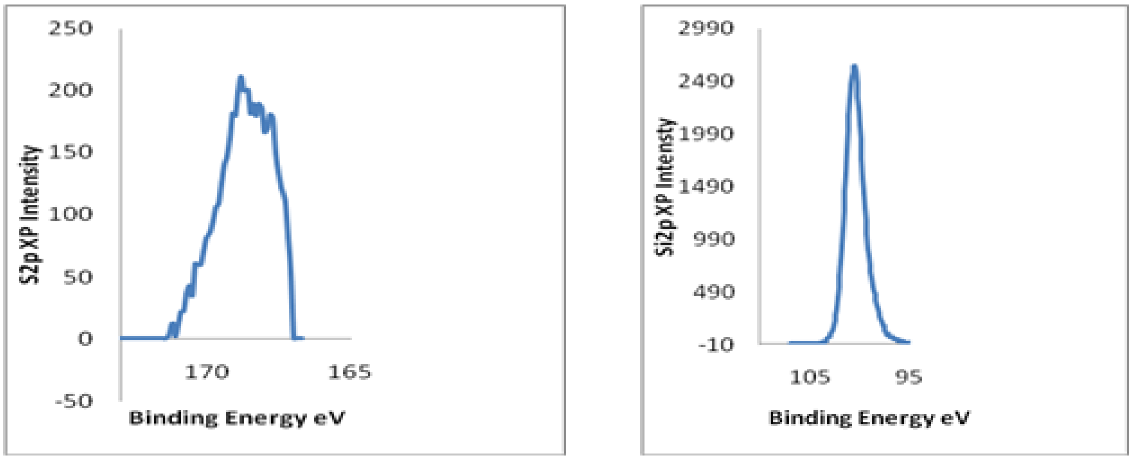

Figure 9: XPS spectra of S2p and Si2p for MT-RHS and sulfonic functionalised MT-RHS.

Catalysts activity

The activity of MTS-based solid acid catalysts for esterification reactions was investigated. Initially, acetic acid and butanol at 110 °C were used as model reagents to investigate the effectiveness of the synthesised catalysts. In addition, the unfunctionalised MTS/MT-RHS were examined to see whether the solid support played a role in the esterification reaction. The unfunctionalised mesoporous support was found to have no contribution to the acidity of the synthesised catalyst because no acetic acid conversion occurred after six hours of reaction time. Moreover, the elemental analysis of the parent RHS and MTS confirmed absence of transition metal contaminants as reported for these materials in previous studies (Elimbinzi *et al.,* 2020, 2018). The conversion of acetic acid by the sulfonic acid functionalised catalysts was found to be 96 and 86% for SO_3H-MTS and SO_3H-MT-RHS, respectively indicating the catalytic action in the esterification reaction (Figure 10).

Both SO_3H-MTS and SO_3H-MT-RHS catalysts were studied further for the esterification reaction of other carboxylic acids (hexanoic acid, lauric acid, palmitic acid, and ricinoleic acid) with butanol at 110 °C (Figure 10-12). When comparing the activity of the two synthesised sulfonic acid functionalised mesoporous silica materials on esterification of different fatty acids, the SO_3H-MTS afforded the highest conversion. For instance, SO_3H-MTS catalyst gave the highest acid conversion of 96% for C2 compared to SO_3H-MT-RHS catalyst, which had 86% for the same acid. Furthermore, the conversion of ricinoleic acid (C18), the longest chain fatty acids used, was higher with SO_3-MTS (42%) compared to SO_3H-MT-RHS for which conversion was 37%. The observed variation in catalytic performance could be due to a difference in the percentage of sulfur content as detected by XPS analysis. The sulfur undergoes oxidation to sulfonic acid, hence improving the catalytic activity. Furthermore, as shown in Table 1, the acid loading of the SO_3H-MTS (1.73 mmol g^{-1}) was greater than that of the SO_3H-MT-RHS (0.15 mmol g^{-1}). However, as the length of the acid chain increased, all catalysts showed a decrease in the conversion of carboxylic acid to the corresponding esters (Tables 2 and 3) corroborating previously reported trends (Elimbinzi and Nyandoro 2021; Osatiashtiani *et al.,* 2016; Liu *et al.,* 2006). However, their effectiveness were generally lower than their counterpart sulfonated zirconia (Elimbinzi and Nyandoro 2021; Osatiashtiani *et al.,* 2016).

The turn over frequency (TOF), which is a quantification of the instantaneous catalytic activity was also calculated, the results of which are presented in Table 2 and 3. The calculation of initial rates of the reactions for both catalysts was in the unit of mmol of the acid consumed per hour. The measurements of initial rates involved at the initial period of reaction up to a period of one hour. The TOFs for the esterification of acetic acid with butanol were 10.3 and 127.7 h^{-1} when SO_3H-MTS and SO_3H-MT-RHS catalysts were used, respectively, which then decreased to 1.0 and 34.4 h^{-1} for the respective catalyst during esterification of ricinoleic acid (Table 2 and 3). Expectedly, TOF, acid conversion and initial reaction rate of reactions also decreased as the carboxylic chain length increased as previously reported (Elimbinzi and Nyandoro 2021; Osatiashtiani *et al.,* 2016; Liu *et al.,* 2006). Various environmentally benevolent modified solid acid catalysts similar to SO_3H-MT-RHS for instance, have been successfully applied in esterification reaction (Diamantopoulos 2015; El Kadib *et al.,* 2013; Sharma *et al.,* 2011; Melero *et al.,* 2010; Zhang *et al.,* 2010; Park *et al.,* 2008). Generally, the use of such solid acid catalysts for esterification reaction have afforded production of esters including those intended for biodiesel production with significant yields (Balan *et al.,* 2021; Mendaros *et al.,* 2020; Shagufta *et al.,* 2017; Saravanan *et al.,* 2014 Melero *et al.,* 2010; Park *et al.,* 2010; Melero *et al.,* 2009; Kulkarni et al. 2006). It is therefore anticipated that, these castor oil-templated mesoporous sulfonic acid modified catalysts could be deployed in biodiesel manufacturing and other esterification reactions.

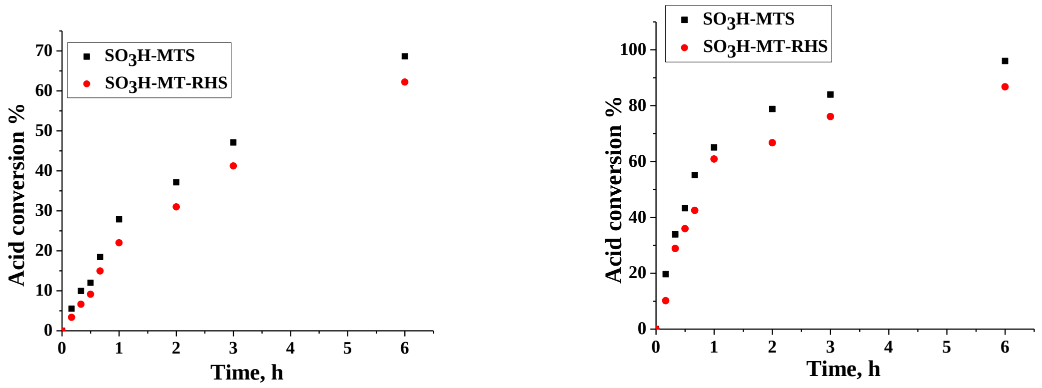

Figure 9: Reaction profiles of acetic (left) and hexanoic (right) acid conversion with butanol at 110 °C.

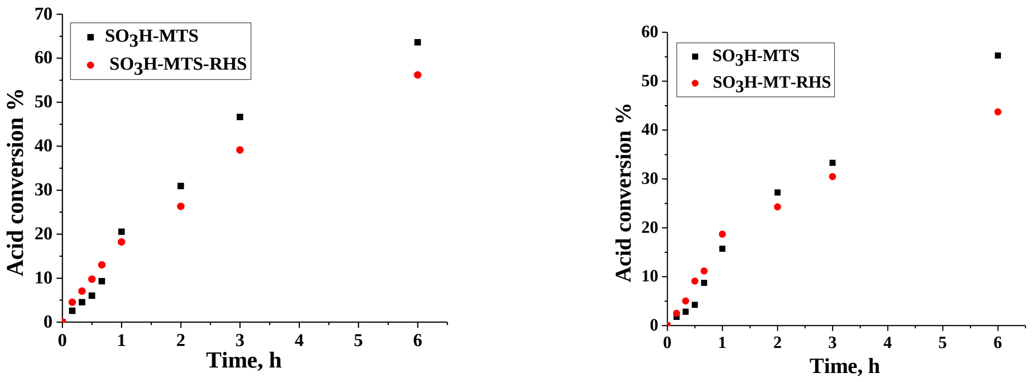

Figure 10: Reaction profiles of lauric (left) and palmitic (right) acid conversion with butanol at 110 °C.

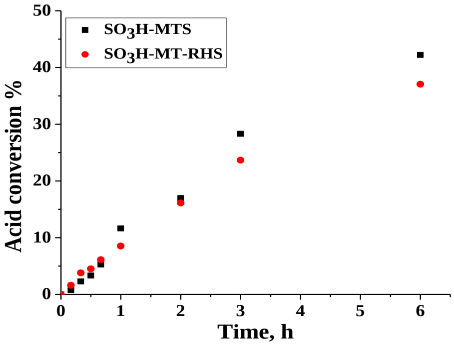

Figure 11: Reaction profiles of ricinoleic acid conversion with butanol at 110 °C.

Table 2: Esterification of different carboxylic acid with butanol over SO_3H-MTS catalyst at 110 °C

Carboxylic acid	6 h conversion (%)	Initial rate (mmol/h)	TOF (h^{-1})
Acetic acid	96	1.78	10.3
Hexanoic acid	68.7	0.79	4.5
Lauric acid	63.6	0.38	2.3
Palmitic acid	55.2	0.34	2.0
Ricinoleic acid	42.2	0.18	1.0

Table 3: Esterification of different carboxylic acid with butanol over SO_3H-MT-RHS catalyst at 110 °C

Carboxylic acid	6 h conversion (%)	Initial rate (mmol/h)	TOF (h^{-1})
Acetic acid	86.8	1.92	127.7
Hexanoic acid	62.2	1.51	100.3
Lauric acid	56.2	1.17	77.7
Palmitic acid	43.7	0.86	57.6
Ricinoleic acid	37.7	0.52	34.4

CONCLUSION

Synthesis of mesoporous support materials using the castor oil as the surfactant and rice husk as the source of silica alongside TOES for comparison was successfully achieved. The synthesised materials were characterised for their porosity characteristics, which exhibited mesoporous features. The mesoporous catalyst support and their derived acid catalysts can therefore successfully be synthesised using the naturally occurring surfactant (castor oil) and rice husk as a source of silica for the purpose of theirvalue addition and mitigation of consequential environmental impacts arising from artificial surfactants and silica sources. The synthesised sulfonic acid functionalised catalysts displayed good catalytic activities for esterification with performance ranging from 96-37% for C2-C18 with butanol at 110 °C within 6 h. Therefore, it is contemplated that such castor oil-templated mesoporous sulfonic acid modified catalysts can be applied in biodiesel production upon process optimisation.

ACKNOWLEDGMENTS

Authors are grateful to Leverhulme Royal Society African Award Phase II and Mkwawa University College of Education for financial support. We are thanksful to Prof. Karen Wilson and Prof. Adam F. Lee group at European Bioenergy Research Institute (EBRI), Aston University, Birmingham, United Kingdom for cordial support during undertakings of this work.

REFERENCES

Alexander M.R., Thompson G.E. and Beamson G. (2000). Characterization of the oxide / hydroxide surface of aluminium using x-ray photoelectron spectroscopy : A procedure for curve fitting the O 1s core level. *Surf. Interface Anal*. **477**:468-477.

Balan W.S., Janaun J., Chung C.H., Semilin V., Zhu Z., Haywood S.K., Touhami D., Chong K.P., Yaser A.Z., Lee P.C. and Zein S.H. (2021). Esterification of residual palm oil using solid acid catalyst derived from rice husk. *J. Hazard. Mater*. 404: Part B, 124092.

Beck J.S., Vartuli J.C., Roth W.J., Leonowicz M.E., Kresge C.T., Schmitt K.D., Chu C.T.W., Olson D.H,, Sheppard E.W., McCullen S.B., Higgins J.B., and Schlenker J.L. (1992). A new family of mesoporous molecular sieves prepared with liquid crystal templates. *J. Am. Chem. Soc*. **114**:10834-10843.

Bhagiyalakshmi M., Ganesh M., Peng M., Vinoba M., Yonglee S. and Taejang H. (2010). Utilization of rice husk ash as silica source for the synthesis of mesoporous KIT-6 and its application to CO_2 adsorption through TREN/TEPA grafting. *Proceedings of the 3rd International Conference on Environmental Technology and Knowledge Transfer*.

Bhagiyalakshmi M., Yun L.J., Anuradha R. and Jang H.T. (2010). Synthesis of chloropropylamine grafted mesoporous MCM-41 , MCM-48 and SBA-15 from rice husk ash : their application to CO_2 chemisorption. *J. Porous Mater*.

17(4):475-484.

Bharti C., Gulati N., Nagaich U. and Pal A, (2015). Mesoporous silica nanoparticles in target drug delivery system: A review. *Int. J. Pharm. Investig*. **5**(3):124-133.

Che S., Garcia-Bennett A.E., Yokoi T., Sakamoto K,, Kunieda H., Terasaki O. and Tatsumi T. (2003). A novel anionic surfactant templating route for synthesizing mesoporous silica with unique structure. *Nat. Mater*. **2**(12):801-805.

Cheng Y-R., Lin H-P. and Mou C-Y. (1999). Control of mesostructure and morphology of surfactant-templated silica in a mixed surfactant system. *Phys. Chem.* **1**(21):5051-5058.

Diamantopoulos N, (2015). Comprehensive review on the biodiesel production using solid acid heterogeneous catalysts. *J. Thermodyn. Catal*. **6**(1):1-8.

Elimbinzi E. and Nyandoro S.S. (2021). Biodiesel production by esterification of ricinoleic acid over a series of synthesized sulfated zirconia catalysts. *Tanz. J. Sci*.**47**(2):812-825.

Elimbinzi, E., Nyandoro S.S., Mubofu E.B., Manayil J.C., Lee A.F. and Wilson K. (2020). Valorization of rice husk silica waste: Organo-amine functionalized castor oil templated mesoporous silicas for biofuels synthesis. *Microporous and Mesoporous Mater.* 294:109868.

Elimbinzi E., Nyandoro S.S., Mubofu E.B., Osatiashtiani A., Manayil J.C., Isaacs M.A., Lee A.F. and Wilson K. (2018). Synthesis of amine functionalized mesoporous silicas templated by castor oil for transesterification. *MRS Adv.* **3**(38):1-9.

Gérardin C., Reboul J., Bonne M. and Lebeau B. (2013). Ecodesign of ordered mesoporous silica materials. *Chem. Soc. Rev*. **42**(9):4217-4255.

Hasanzadeh M., Shadjou N., Guardia M., Morteza E. and Peyman S. (2012). Mesoporous silica-based materials for use in biosensors. *TrAC - Trends in Anal. Chem.* **33**:117–29.

He Q. and Shi J. (2011). Mesoporous silica nanoparticle based nano drug delivery systems: synthesis, controlled drug release and delivery, pharmacokinetics and biocompatibility. *J.Mater. Chem.* **21**(16):5845.

Hughes A.E. and Sexton B.A. (1988). Curve fitting XPS spectra. *J. Electron Spectros Relat Phenomena* **46**:31-42.

Jothiramalingam R. and Wang M.K. (2009). Review of recent developments in solid acid, base, and enzyme catalysts (heterogeneous) for biodiesel production via transesterification. *Ind. Eng. Chem. Res*.**48**(13): 6162-6172.

El Kadib A., Finiels A., and Brunel D. (2013). Sulfonic acid functionalised ordered mesoporous materials as catalysts for fine chemical synthesis. *Chem. Commun*. **49**(80): 9073-9076.

Kresge C.T., Leonowicz, M.E,, Roth W.J., Vartuli J.C. and Beck J.S. (1992). Ordered mesoporous molecular sieves synthesized by liquid-crystal template mechanism. *Nature*. **359**:710-712.

Kulkarni M.G., Gopinath R., Meher L.C. and Dalai A.K. (2006). Solid acid catalyzed biodiesel production by simultaneous esterification and transesterification. *Green Chem*. **8**(12):1056–1062.

Ligate F.J. and Mdoe J.E.G. (2015). Removal of heavy metal ions from aqueous solution using rice husks-based adsorbents. *Tanz. J. Sci*. **41**(1):90-102.

Liu, F., Kuan H., Zheng A., Feng S.X. and Sheng D. (2018). “Hydrophobic solid acids and their catalytic applications in green and sustainable chemistry.” *ACS Catalysis* **8**(1):372–391.

Liu Y., Lotero E. and Goodwin J.G. (2006). Effect of carbon chain length on esterification of carboxylic acids with methanol using acid catalysis. *J. Catal.* **243**(2):221-228.

López D.E., Goodwin J.G., Bruce D.A., Furuta S. (2008). Esterification and transesterification using modified-zirconia catalysts. *Appl. Catal. A Gen*. **339**(1):76-83.

Medina-Juarez O., Garcia-Sanchez M.A., Arellano-Sanchez U., Kornhauser-Straus I. and Rojas-Gonzalez F. (2016). Optimal surface amino-functionalization following thermo-alkaline treatment of nanostructured silica adsorbents for enhanced CO_2 adsorption. *Materials*. **9**(898):1-24.

Meghshyam K.. Patil N., Prasad A.M. and Reddy B. (2011). Zirconia-based solid acids: Green and heterogeneous catalysts for organic synthesis. *Curr. Org. Chem*.**15**(23):3961-3985.

Melero J.A., Bautista L.F., Morales G., Iglesias J. and Sánchez-Vázquez R. (2010). Biodiesel production from crude palm oil using sulfonic acid-modified mesostructured catalysts. *Chem. Eng. J*.**161**(3):323-331.

Melero J.A., Iglesias J. and Morales G. (2009). Heterogeneous acid catalysts for biodiesel production: current status and future challenges. *Green Chem*.**11**(9):1285.

Mendaros C.M., Go A.W., Nietes W.J.T., Gollem B.E.J.O. and Cabatingan L.K. (2020). Direct sulfonation of cacao shell to synthesize a solid acid catalyst for the esterification of oleic acid with methanol. *Renew Energy*. **152**:320-330.

Narkhede N. and Patel A. (2013). Biodiesel production by esterification of oleic acid and transesterification of soybean oil using a new solid acid catalyst comprising 12-tungstosilicic acid and zeolite Hβ *Ind. Eng. Chem. Res*. **52**(38):13637-13644.

Osatiashtiani A., Durndell L.J., Manayil J.C., Lee A.F. and Wilson K. (2016). Influence of alkyl chain length on sulfated zirconia catalysed batch and continuous esterification of carboxylic acids by light alcohols. *Green Chem*.;**18**(20):5529-5535.

Pagar O.B., Nagare H.S., Chine Y.M., Autade R.R., Narode P.R. and Sanklecha V.M. (2018). Mesoporous silica: A review. *Inter. J. Pharmac. Drug Analysis* **6**:1-12.

Park Y.M., Lee D.W., Kim D.K., Lee J.S. and Lee K.Y. (2008). The heterogeneous catalyst system for the continuous conversion of free fatty acids in used vegetable oils for the production of biodiesel. *Catal Today*.**131**(1-4):238-243.

Park Y.M., Lee J.Y., Chung S.H., Park I.S., Lee S-Y., Kim D-K., Lee J-S. and Lee K-Y. 2010. Esterification of used vegetable oils using the heterogeneous WO_3/ZrO_2 catalyst for production of biodiesel. *Bioresour. Technol*. **101**(1):559-561.

Reddy B.M., Sreekanth P.M. and Reddy V.R. (2005). Modified zirconia solid acid catalysts for organic synthesis and transformations. *J. Mol. Catal. A Chem*. **225**(1):71-78.

Ritter H., Ramm J.H. and Brühwiler D. (2010). Influence of the structural properties of mesoporous silica on the adsorption of guest molecules. *Materials*. **3**(8):4500-4509.

Saravanan K., Tyagi B. and Bajaj H.C. (2014). Catalytic activity of sulfated zirconia solid acid catalyst for esterification of myristic acid with methanol. *Indian J. Chem. -Sec A*. **53**(7):799-805.

Shagufta, Ahmad I. and Dhar R. (2017). Sulfonic acid-functionalized solid acid catalyst in esterification and transesterification reactions. *Catal. Surv.Asia*. **21**(2):53-69.

Sharma Y.C., Singh B. and Korstad J. (2011). Advancements in solid acid catalysts for ecofriendly and economically viable synthesis of biodiesel. *Biofuels, Bioprod Biorefining*. **5**(1):69-92.

Tang F., Linlin L. and Dong C. (2012). Mesoporous silica nanoparticles: Synthesis, biocompatibility and drug delivery. *Adv. Mater.* **24**(12):1504-1534.

Vaisman B., Shikanov A. and Domb A.J. (2008). The Isolation of Ricinoleic Acid from Castor Oil by Salt-Solubility-Based Fractionation for the Biopharmaceutical Applications. *J. Am. Oil Chem. Soc.* **85**(2):169-184.

Zhang J., Shangxing C., Rui Y. and Yuanyuan Y. (2010). Biodiesel Production from vegetable oil using heterogenous acid and alkali catalyst. *Fuel* **89**(10):2939-2944.

Zhao D., Sun J., Li Q., Stucky G.D., and Santa Barbara, (2000). Morphological control of highly ordered mesoporous silica SBA-15 *Chem. Mater*. **12**(2):275–279.